

# PHOTONICS Research

## Graphene-decorated microfiber knot as a broadband resonator for ultrahigh-repetition-rate pulse fiber lasers

MENG LIU,<sup>1,2</sup> RUI TANG,<sup>1</sup> AI-PING LUO,<sup>1,2</sup>  WEN-CHENG XU,<sup>1,2,3</sup> AND ZHI-CHAO LUO<sup>1,2,\*</sup> 

<sup>1</sup>Guangdong Provincial Key Laboratory of Nanophotonic Functional Materials and Devices & Guangzhou Key Laboratory for Special Fiber Photonic Devices and Applications, South China Normal University, Guangzhou 510006, China

<sup>2</sup>Guangdong Provincial Engineering Technology Research Center for Microstructured Functional Fibers and Devices, South China Normal University, Guangzhou 510006, China

<sup>3</sup>e-mail: xuwch@scnu.edu.cn

\*Corresponding author: zcluo@scnu.edu.cn

Received 17 May 2018; revised 7 June 2018; accepted 7 June 2018; posted 7 June 2018 (Doc. ID 331700); published 26 July 2018

Searching for an ultrahigh-repetition-rate pulse on the order of hundreds of gigahertz (GHz) is still a challenging task in the ultrafast laser community. Recently, high-quality silicon/silica-based resonators were exploited to generate a high-repetition-rate pulse based on the filter-driven four-wave mixing effect in fiber lasers. However, despite their great performance, the silicon/silica-based resonators still have some drawbacks, such as single waveband operation and low coupling efficiency between the fiber and resonators. To overcome these drawbacks, herein we proposed an all-fiber broadband resonator fabricated by depositing the graphene onto a microfiber knot. As a proof-of-concept experiment, the graphene-deposited broadband microfiber knot resonator (MKR) was applied to Er- and Yb-doped fiber lasers operating at two different wavebands, respectively, to efficiently generate hundreds-of-GHz-repetition-rate pulses. Such a graphene-deposited broadband MKR could open some new applications in ultrafast laser technology, broadband optical frequency comb generation, and other related fields of photonics. © 2018 Chinese Laser Press

**OCIS codes:** (190.4400) Nonlinear optics, materials; (140.3510) Lasers, fiber; (140.4050) Mode-locked lasers; (190.4380) Nonlinear optics, four-wave mixing.

<https://doi.org/10.1364/PRJ.6.0000C1>

### 1. INTRODUCTION

Ultrafast lasers have attracted intensive interest due to their various applications in fields from fundamental science to industrial purposes [1,2]. In particular, the all-fiber ultrafast lasers possess inherent advantages such as excellent heat dissipation, flexible light path, and compact design, which provide an outstanding platform for generating ultrashort pulses [3]. As one key parameter of ultrafast fiber lasers, the pulse repetition rate is vital to their application. The high-repetition-rate pulse could find versatile applications, i.e., optical communication systems and microwave photonics [4,5]. Thus, there is always a strong motivation to develop ultrafast fiber lasers with pulse repetition rates from the order of gigahertz (GHz) to hundreds of GHz. So far, various approaches have been proposed to achieve high-repetition-rate pulses in fiber lasers. A direct approach to obtain high-repetition-rate pulses in fiber lasers is to reduce the cavity length. Recent achievements have shown that ~20 GHz could be obtained from a short-cavity fiber laser [6]. However, for higher-repetition-rate pulses in fiber lasers, i.e., on the order

of 100 GHz, this would be hard to reach by simply reducing the cavity length. Therefore, there is great motivation for discovering new methods for generation of ultrahigh-repetition-rate pulses on the order of 100 GHz.

In fact, as a promising method, the dissipative four-wave-mixing (DFWM) mode-locking technique has been proposed to effectively achieve ultrahigh-repetition-rate pulses (over 100 GHz) in fiber lasers [7–11]. The key devices to generate DFWM mode-locked pulses in an ultrafast laser are multi-wavelength selective components and highly nonlinear elements with proper dispersion parameters. Very recently, Peccianti *et al.* proposed an integrated optical device, namely, a silica-based microring resonator, to obtain a 200 GHz pulse train in a fiber laser [12]. A great advance is that the microring resonator combines two functions of the comb filtering and highly nonlinear effects [12–20] for DFWM mode locking [12,21–25], which they termed as filter-driven FWM (FD-FWM) [12]. However, for effective generation of the FWM effect, the cross section of the silicon/silica-based microring resonator needs to be carefully designed to control the dispersion parameter, which makes

the microring resonator difficult for broadband operation. Therefore, a single silicon/silica-based resonator generally only operates at a specific waveband. Moreover, it is still challenging to reach stable and highly efficient coupling between the fiber and the silicon/silica-based resonator unless the fiber is carefully aligned [12,16]. Thus, it is of great significance to develop an all-fiber resonator with broadband operation for ultrahigh-repetition-rate pulse fiber lasers based on the DFWM mode-locking technique.

Over the last decade, two-dimensional (2D) materials including graphene [26], transition metal dichalcogenides (TMDs) [27], topological insulators [28], black phosphorus [29], and MXene [30] have attracted more and more attention due to their excellent optical, electronic, and electrochemical characteristics. In the fields of ultrafast and nonlinear photonics, generally the 2D materials were employed to fabricate the broadband saturable absorbers (SAs) or nonlinear elements since they possess broadband saturable absorption and a large nonlinear refractive index [31–35]. To date, ultrafast fiber lasers based on different types of 2D-material SAs have been demonstrated [30,36–48]. Therefore, the 2D materials could be considered as good candidates for the fabrication of compact ultrafast fiber lasers. Among these 2D materials, graphene is the most highly studied. It was demonstrated that graphene possesses not only saturable absorption, but also remarkably large third-order optical susceptibility, which is weakly dependent on the operation waveband [31,49,50]. Therefore, the graphene could potentially be used to generate the broadband FWM effect [26,31,49,51,52]. Herein, by virtue of the excellent nonlinear optical response of graphene, we proposed a graphene-decorated microfiber knot as the broadband resonator for generation of the FWM effect. With the fabricated graphene-deposited microfiber knot resonator (MKR), DFWM mode-locked Er-doped fiber (EDF) and Yb-doped fiber (YDF) lasers delivering ultrahigh-repetition-rate pulses were demonstrated. Note that our scheme relies on the highly nonlinear effects provided by the graphene-deposited MKR. Therefore, we also refer to the mode-locking technique as FD-FWM here. The 106.7- and 162-GHz-repetition-rate pulses were obtained at 1.55  $\mu\text{m}$  and 1.06  $\mu\text{m}$  wavebands, respectively. The achieved results demonstrated that the graphene-deposited microfiber knot could be a good candidate as a broadband resonator for DFWM mode-locking fiber lasers and also would open some new opportunities of MKR for applications in various fields.

## 2. FABRICATION AND CHARACTERISTICS OF GRAPHENE-DEPOSITED MKR

### A. MKR Preparation

Using the flame-brushing technique [53], the standard single-mode fiber (SMF) was stretched into microfiber with diameter of  $\sim 5 \mu\text{m}$ . Then we manually knotted the waist of the microfiber into a knot with a diameter of 578  $\mu\text{m}$ , as presented in Fig. 1(a). Two sections of free SMF still remained at both ends of the knot when the fabrication of MKR was completed, which makes the MKR more stable and fiber-integrable.

### B. Graphene-Deposited MKR Fabrication

The graphene-deposited MKR was fabricated by using the optical deposition method [54,55]. The light source is an amplified spontaneous emission (ASE). We injected light into the MKR and dropped the prepared graphene/dimethylformamide solution with a concentration of 0.07 mg/mL onto the glass slice until the solution submerged the MKR. By virtue of the optical force provided by the light source, the graphene could be readily coated on the MKR. The whole process was *in situ* monitored by a microscope with a 100-fold magnification. When the deposition amount of graphene was appropriate, the light source was turned off to stop the deposition process. Here the deposition length was  $\sim 130 \mu\text{m}$ , which was optimized for better performance of the fiber lasers. After taking out the residual solution, the fabrication of the graphene-deposited MKR was accomplished, as shown in Fig. 1(b). It can be seen that graphene has been well deposited onto the MKR. As presented in Fig. 1(c), the scattering evanescent field could be observed around the MKR when the visible light was injected. Here, the insertion loss of the graphene-deposited MKR is  $\sim 5.4 \text{ dB}$ .

To check the spectral response of the graphene-deposited MKR, we employ an ASE light source operating at a 1.55- $\mu\text{m}$  waveband as the input. The red solid line in Fig. 2 shows the measured spectral response of the graphene-deposited MKR. Here, the free spectral range (FSR) of the MKR is 0.86 nm at 1.55  $\mu\text{m}$ . As we know, the spectral response of the MKR is defined by its diameter [56,57]. Therefore, the FSR of the proposed MKR with a diameter of 578  $\mu\text{m}$  is calculated to be 0.86 nm. For comparison, we have also provided the calculated spectral responses in Fig. 2 with blue dotted curves, where we can see that experimental result is consistent with the theoretical one. Note that the  $Q$ -factor of the graphene-deposited MKR is calculated to be  $\sim 5962$ , which could be further increased by improving the quality of the MKR.

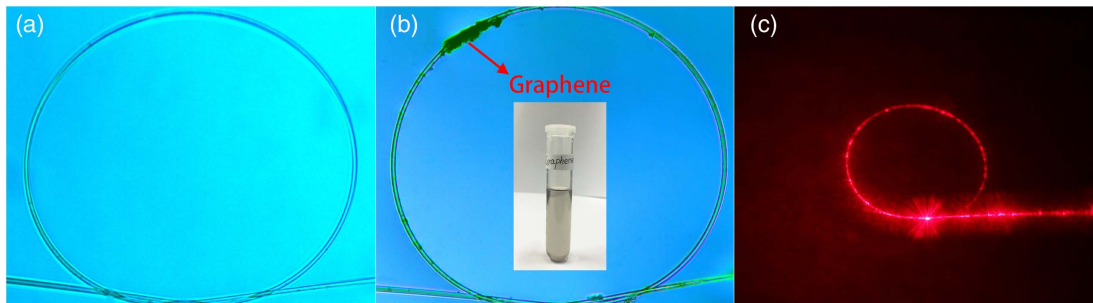


**Fig. 1.** (a) Microscopy image of the fabricated MKR; (b) microscopy image of the graphene-deposited MKR; (c) scattering evanescent field along the graphene-deposited MKR.

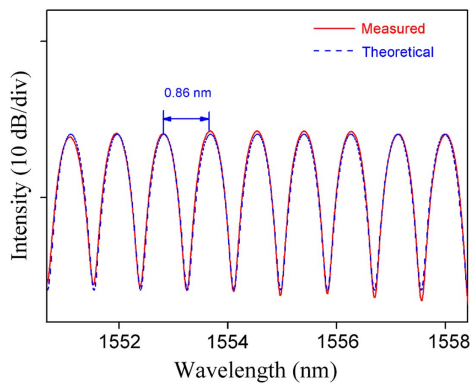


**Fig. 2.** Spectral response of the graphene-deposited MKR. Red solid line, measured spectral response of the graphene-deposited MKR; blue dotted line, theoretically calculated spectral response of the graphene-deposited MKR.

### 3. LASER SETUP AND PERFORMANCE

In order to investigate the performance of the broadband MKR for FD-FWM mode-locking operation in fiber lasers, we constructed the fiber-ring laser based on such a device, as shown in Fig. 3. First, the 7-m EDF with a dispersion parameter of  $-17.3 \text{ ps} \cdot \text{km}^{-1} \cdot \text{nm}^{-1}$  was used as the active gain medium for 1.55- $\mu\text{m}$  waveband operation. The other fibers are all SMFs. The total cavity length is 28.8 m, resulting in a main cavity longitudinal mode spacing of 7.09 MHz. Note that the net dispersion of the EDF laser is  $\sim -0.32 \text{ ps}^2$ . Two polarization controllers (PCs) were employed to adjust the polarization state. Unidirectional operation was ensured by a polarization-independent isolator (PI-ISO). The laser was taken out by a 10% coupler. An optical spectrum analyzer and a commercial autocorrelator (FR-103XL) were employed to monitor the laser performance.

During the process of increasing the pump power, it was found that the lasing threshold was  $\sim 20 \text{ mW}$ . However, in this case only the unstable single-wavelength operation could be observed. Then the pump power was carefully tuned to about 198 mW, and the PCs were slightly adjusted. A notable phenomenon was that several stable lasing lines could be observed on the spectrum. By further optimizing the laser operation, up to 6 stable lasing wavelengths were obtained, as shown in Fig. 4(a). The spectral spacing is 0.86 nm, which is defined

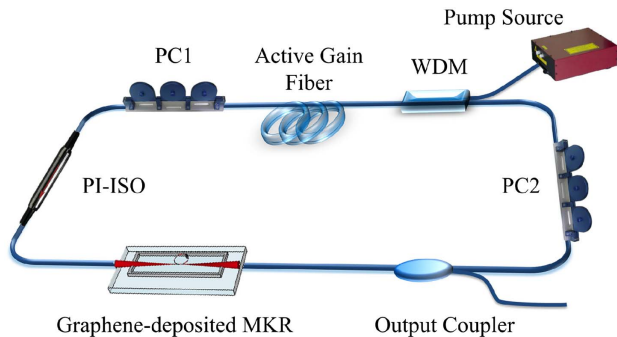


**Fig. 3.** Schematic of the ultrafast fiber laser used in the experiment.

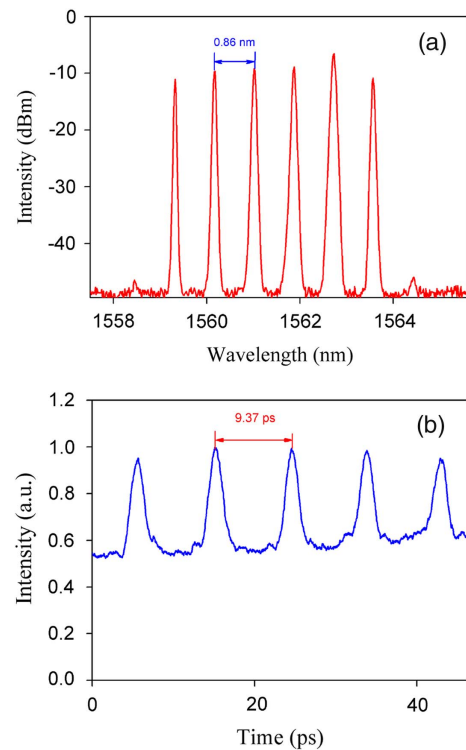


**Fig. 4.** FD-FWM mode-locking operation in the EDF laser based on graphene-deposited MKR. (a) Output spectrum; (b) corresponding autocorrelation trace.

by the FSR of the MKR. Note that the shape of the spectral envelope is not a typical DFWM mode-locking one, which might be due to the existence of the cascading FWM effect in the laser cavity. However, the spectral envelope could be shaped by properly rotating the PCs. The stable operation of multiwavelength lasing lines indicates that the FD-FWM mode-locking operation has been achieved by the graphene-deposited MKR. From the spectral spacing of 0.86 nm, it can be deduced that the FD-FWM mode-locking operation possesses a pulse repetition rate of  $\sim 106.7 \text{ GHz}$ . Thus, the current state-of-the-art oscilloscope could not check the pulses due to the limited bandwidth. To measure the pulse signal of the FD-FWM mode locking, an autocorrelator was employed. As presented in Fig. 4(b), the pulse-to-pulse interval is  $\sim 9.37 \text{ ps}$ , demonstrating that the pulse repetition rate of 106.7 GHz has been obtained. Here, the noise level of the autocorrelation trace is high, indicating that the mode-locking quality is not good enough. However, it is believed that the noise level of the autocorrelation trace could be suppressed by selecting a graphene-decorated high- $Q$  microring resonator or increasing the spacing of the cavity fundamental modes [12]. Note that we have also increased the pump power to above 200 mW. However, in this case the mode-locked pulse became unstable. To verify the stability of the proposed FD-FWM mode-locked fiber laser, we repeatedly scanned the laser output for 100 min with a 5-min interval. Figure 5(a) shows the scanned results. No significant wavelength drifts and power variations for each lasing line were directly observed. For better clarity, we have also shown the power fluctuations of each lasing line in

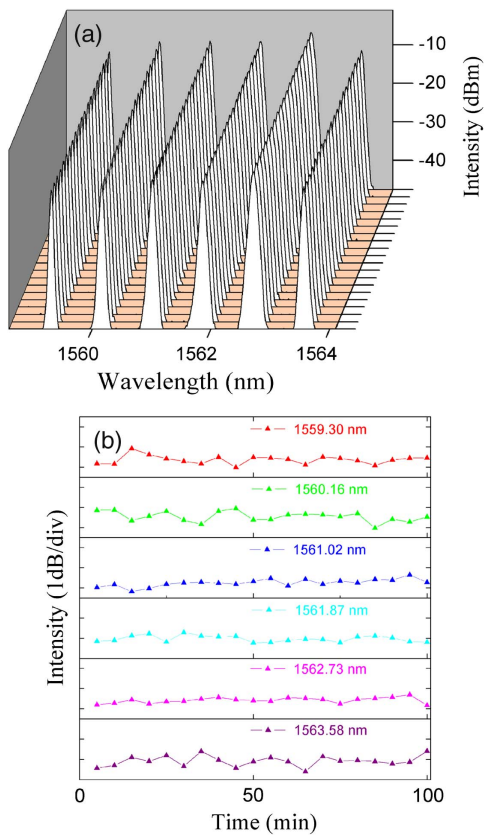


**Fig. 5.** Stability of the proposed FD-FWM mode-locked fiber laser. (a) Repeatedly scanned output; (b) power fluctuation tracking.

Fig. 5(b). Here, the maximum power fluctuation is less than 1 dB. These results indicate that the proposed DFWM mode-locked fiber laser operated stably with the experimental conditions.

As mentioned above, the nonlinear optical response of graphene is weakly dependent on wavelength, which could be used to generate the FWM effect at different wavebands [26,31,49,51,52]. Therefore, to gain a further insight into the broadband operation of the graphene-deposited MKR, we replaced the EDF by the YDF as well as the corresponding optical components to investigate the ultrahigh-repetition-rate pulse generation at a 1.06- $\mu\text{m}$  waveband based on the proposed graphene-microfiber device. For low-loss design at the 1.06- $\mu\text{m}$  waveband, in this case the HI-1060 fiber was drawn into a microfiber and fabricated into a knot structure. The FSR of the graphene-deposited MKR is 0.59 nm. When the as-prepared graphene-deposited MKR was inserted into the YDF laser, the stable FD-FWM mode-locking operation could be also obtained after proper adjustments of cavity parameters. Here, the cavity length is 30.2 m and the net cavity dispersion is  $\sim 0.67 \text{ ps}^2$ . Thus, the spacing of the main cavity modes is 6.82 MHz. The laser performance is summarized in Fig. 6. Four stable lasing lines centered at 1044.8 nm were obtained. The channel spacing is 0.59 nm, corresponding to a 162-GHz repetition rate of the pulse train, as presented in Fig. 6(a). The measured autocorrelation trace shows the pulse interval is 6.17 ps, which is in good agreement with the channel spacing of the FWM mode-locking operation, as depicted in Fig. 6(b). The examination of stable operation also demonstrated that the FD-FWM mode-locked YDF laser operated stably, as shown in Figs. 6(c) and 6(d).

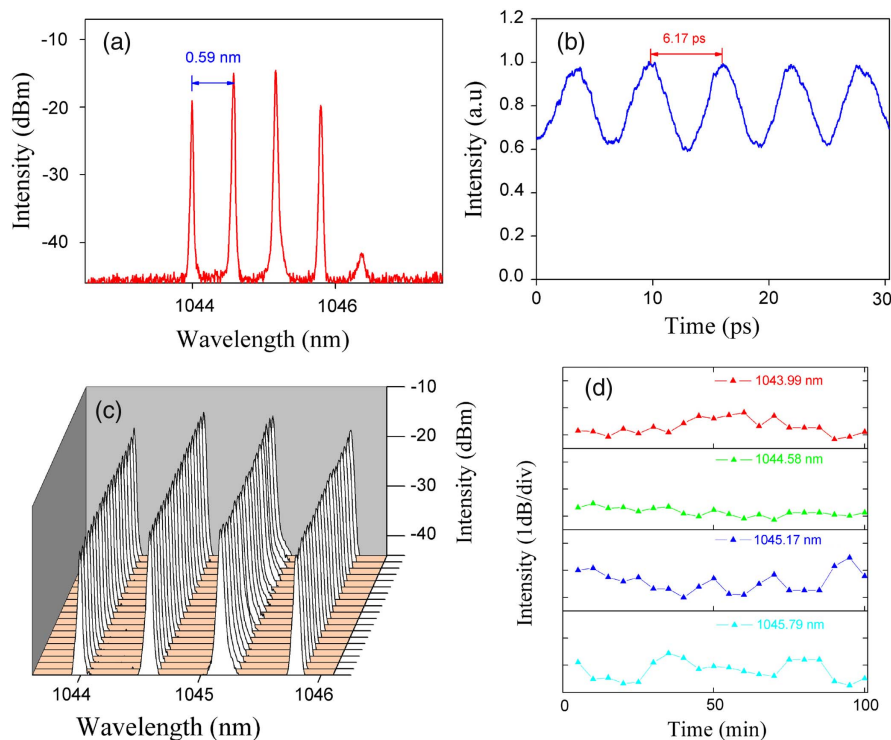


**Fig. 6.** FD-FWM mode-locking operation in the YDF laser based on graphene-deposited MKR. (a) Output spectrum; (b) autocorrelation trace; (c) repeatedly scanned output 20 times with a 5-min interval; (d) power fluctuation of each lasing line within 100 min.

## 4. DISCUSSION

In the experiment, there exist pedestals on the autocorrelation traces of the FD-FWM mode-locked pulse both in the 1.55  $\mu\text{m}$  and 1.06- $\mu\text{m}$  wavebands based on the proposed graphene-deposited MKR. This is because the bandwidth of each filtering channel of the graphene-deposited MKR is large, which allows multiple-cavity longitudinal modes at the lasing wavelengths. For example, the spacing of the main cavity modes is 7.09 MHz for EDF laser, and the bandwidth of the lasing line of the graphene-deposited MKRs for EDF laser is 7.4 GHz. Thus, it is inferred that it allowed  $\sim 1043$  cavity longitudinal modes at the lasing wavelengths for the EDF laser. The multiple-cavity longitudinal modes inside the lasing lines would lead to the supermode instability problem [21,58–60], which mainly degenerates the laser performance. To prove it, we have measured the radio frequency (RF) spectrum corresponding to the status of Fig. 4. In this case, the peaks could be seen at the locations of harmonics of the cavity repetition rate, showing that the fiber laser suffers from supermode instability. A similar case was also observed in the high-repetition-rate pulse YDF laser. However, the experimental results clearly demonstrated that the graphene-coated optical MKR could indeed be employed as a high-performance photonic device to achieve broadband FD-FWM mode-locked operation with an ultrahigh repetition rate. Therefore, the proof-of-concept device represents a step in overcoming the broadband FWM generation of an integrated silicon/silica-based resonator for frequency comb or DFWM mode-locked operation. As an alternative solution, the graphene could be coated on the silicon/silica-based resonators with a high  $Q$ -factor. In this way, the interaction among the propagation light, the graphene, and the silicon/silica-based resonators could provide the conditions for the broadband FWM generation. In the experiment, we have also incorporated an MKR without graphene deposition into the fiber laser. However, no stable multiple lasing modes could be obtained. It further demonstrated that the high nonlinearity induced by the graphene could generate a broadband FWM effect to realize DFWM mode locking at both 1.06- $\mu\text{m}$  and 1.55- $\mu\text{m}$  wavebands. Moreover, graphene also possesses the saturable absorption effect. Note that the saturable absorption effect could modulate the intensities of the lasing lines, which could be used to further stabilize the multiple lasing lines of the fiber lasers. On the other hand, due to the successful demonstration of silicon waveguide amplifiers, including the high-gain-medium-doped micro/nanofiber waveguide lasers [61,62], it is expected that the graphene can be integrated to such silicon waveguide amplifier platforms for more compact design, which provides great opportunities for achieving stable, high-performance laser sources operating at ultrahigh repetition rates.

## 5. CONCLUSION

In summary, we proposed and demonstrated a graphene-decorated MKR to achieve the broadband FWM effect for ultrahigh-repetition-rate pulse generation in EDF and YDF lasers. With the proposed graphene-microfiber photonic device, pulse trains with 162-GHz and 106.7-GHz repetition rates operating at 1.06  $\mu\text{m}$  and 1.55- $\mu\text{m}$  wavebands could be obtained, respectively. We believed that the proof-of-concept

experiments would not only shed new light on the investigations of microring resonators with broadband operation, but also open some important applications of microring resonators in broadband optical frequency comb generation, ultrahigh-repetition-rate pulses created by the DFWM mode-locking technique, and other related fields such as graphene optoelectronics and nonlinear optics.

**Funding.** National Natural Science Foundation of China (NSFC) (11474108, 11304101, 61307058, 61378036); Guangdong Natural Science Funds for Distinguished Young Scholar (2014A030306019); Program for Outstanding Innovative Young Talents of Guangdong Province (2014TQ01X220); Pearl River S&T Nova Program of Guangzhou (2014J2200008); Natural Science Foundation of Guangdong Province (2014A030311037); Program for Outstanding Young Teachers in Guangdong Higher Education Institutes (YQ2015051); Science and Technology Project of Guangdong (2016B090925004); Foundation for Young Talents in Higher Education of Guangdong (2017KQNCX051); Science and Technology Program of Guangzhou (201607010245); Scientific Research Foundation of Young Teacher of South China Normal University (17KJ09).

## REFERENCES

1. U. Keller, "Recent developments in compact ultrafast lasers," *Nature* **424**, 831–838 (2003).
2. M. E. Fermann and I. Hartl, "Ultrafast fibre lasers," *Nat. Photonics* **7**, 868–874 (2013).
3. F. W. Wise, A. Chong, and W. Renninger, "High-energy femtosecond fiber lasers based on pulse propagation at normal dispersion," *Laser Photon. Rev.* **2**, 58–73 (2008).
4. D. Cotter, R. J. Manning, K. J. Blow, A. D. Ellis, A. E. Kelly, D. Nesses, I. D. Phillips, A. J. Poustie, and D. C. Rogers, "Nonlinear optics for high-speed digital information processing," *Science* **286**, 1523–1528 (1999).
5. Z. Y. Zhang, A. E. H. Oehler, B. Resan, S. Kurnulis, K. J. Zhou, Q. Wang, M. Mangold, T. Suedmeyer, U. Keller, K. J. Weingarten, and R. A. Hogg, "1.55  $\mu\text{m}$  InAs/GaAs quantum dots and high repetition rate quantum dot SESAM mode-locked laser," *Sci. Rep.* **2**, 477 (2012).
6. A. Martinez and S. Yamashita, "Multi-gigahertz repetition rate passively mode locked fiber lasers using carbon nanotubes," *Opt. Express* **19**, 6155–6163 (2011).
7. M. Quiroga-Teixeiro, C. B. Clausen, M. P. Sørensen, P. L. Christiansen, and P. A. Andrekson, "Passive mode locking by dissipative four-wave mixing," *J. Opt. Soc. Am. B* **15**, 1315–1321 (1998).
8. S. M. Zhang, F. Y. Lu, X. Y. Dong, P. Shum, X. F. Yang, X. Q. Zhou, Y. D. Gong, and C. Lu, "Passive mode locking at harmonics of the free spectral range of the intracavity filter in a fiber ring laser," *Opt. Lett.* **30**, 2852–2854 (2005).
9. J. Schröder, S. Coen, F. Vanholsbeeck, and T. Sylvestre, "Passively mode-locked Raman fiber laser with 100 GHz repetition rate," *Opt. Lett.* **31**, 3489–3491 (2006).
10. J. Schröder, T. D. Vo, and B. J. Eggleton, "Repetition-rate-selective, wavelength-tunable mode-locked laser at up to 640 GHz," *Opt. Lett.* **34**, 3902–3904 (2009).
11. D. Mao, X. Liu, Z. Sun, H. Lu, D. Han, G. Wang, and F. Wang, "Flexible high-repetition-rate ultrafast fiber laser," *Sci. Rep.* **3**, 3223 (2013).
12. M. Peccianti, A. Pasquazi, Y. Park, B. E. Little, S. T. Chu, D. J. Moss, and R. Morandotti, "Demonstration of a stable ultrafast laser based on a nonlinear microcavity," *Nat. Commun.* **3**, 765 (2012).
13. P. Del'Haye, A. Schliesser, O. Arcizet, T. Wilken, R. Holzwarth, and T. J. Kippenberg, "Optical frequency comb generation from a monolithic microresonator," *Nature* **450**, 1214–1217 (2007).

14. I. S. Grudin, N. Yu, and L. Maleki, "Generation of optical frequency combs with a  $\text{CaF}_2$  resonator," *Opt. Lett.* **34**, 878–880 (2009).
15. J. S. Levy, A. Gondarenko, M. A. Foster, A. C. Turner-Foster, A. L. Gaeta, and M. Lipson, "CMOS-compatible multiple wavelength oscillator for on-chip optical interconnects," *Nat. Photonics* **4**, 37–40 (2010).
16. L. Razzari, D. Duchesne, M. Ferrera, R. Morandotti, S. Chu, B. E. Little, and D. J. Moss, "CMOS-compatible integrated optical hyper-parametric oscillator," *Nat. Photonics* **4**, 41–45 (2010).
17. T. J. Kippenberg, R. Holzwarth, and S. A. Diddams, "Microresonator-based optical frequency combs," *Science* **332**, 555–559 (2011).
18. F. Ferdous, H. Miao, D. E. Leaird, K. Srinivasan, J. Wang, L. Chen, L. T. Varghese, and A. M. Weiner, "Spectral line-by-line shaping of on-chip microring resonator frequency combs," *Nat. Photonics* **5**, 770–776 (2011).
19. A. G. Griffith, R. K. Lau, J. Cardenas, Y. Okawachi, A. Mohanty, R. Fain, Y. H. D. Lee, M. Yu, C. T. Phare, C. B. Poitras, A. L. Gaeta, and M. Lipson, "Silicon-chip mid-infrared frequency comb generation," *Nat. Commun.* **6**, 6299 (2015).
20. A. Pasquazi, M. Peccianti, L. Razzari, D. J. Moss, S. Coen, M. Erkintalo, Y. K. Chembo, T. Hansson, S. Wabnitz, P. Del'Haye, X. Xue, A. M. Weiner, and R. Morandotti, "Micro-combs: a novel generation of optical sources," *Phys. Rep.* **729**, 1–81 (2018).
21. A. Pasquazi, M. Peccianti, B. E. Little, S. T. Chu, D. J. Moss, and R. Morandotti, "Stable, dual mode, high repetition rate mode-locked laser based on a microring resonator," *Opt. Express* **20**, 27355–27363 (2012).
22. S. S. Jyu, L. G. Yang, C. Y. Wong, C. H. Yeh, C. W. Chow, H. K. Tsang, and Y. Lai, "250-GHz passive harmonic mode-locked Er-doped fiber laser by dissipative four-wave mixing with silicon-based micro-ring," *IEEE Photon. J.* **5**, 1502107 (2013).
23. K. Saha, Y. Okawachi, B. Shim, J. S. Levy, R. Salem, A. R. Johnson, M. A. Foster, M. R. Lamont, M. Lipson, and A. L. Gaeta, "Modelocking and femtosecond pulse generation in chip-based frequency combs," *Opt. Express* **21**, 1335–1343 (2013).
24. L. G. Yang, S. S. Jyu, C. W. Chow, C. H. Yeh, C. Y. Wong, H. K. Tsang, and Y. Lai, "A 110 GHz passive mode-locked fiber laser based on a nonlinear silicon-micro-ring-resonator," *Laser Phys. Lett.* **11**, 065101 (2014).
25. W. Wang, W. Zhang, S. T. Chu, B. E. Little, Q. Yang, L. Wang, X. Hu, L. Wang, G. Wang, Y. Wang, and W. Zhao, "Repetition rate multiplication laser source based on a microring resonator," *ACS Photon.* **4**, 1677–1683 (2017).
26. F. Bonaccorso, Z. Sun, T. Hasan, and A. C. Ferrari, "Graphene photonics and optoelectronics," *Nat. Photonics* **4**, 611–622 (2010).
27. Q. H. Wang, K. Kalantar-Zadeh, A. Kis, J. N. Coleman, and M. S. Strano, "Electronics and optoelectronics of two-dimensional transition metal dichalcogenides," *Nat. Nanotechnol.* **7**, 699–712 (2012).
28. M. Z. Hasan and C. L. Kane, "Colloquium: topological insulators," *Rev. Mod. Phys.* **82**, 3045–3067 (2010).
29. L. Li, Y. Yu, G. Ye, Q. Ge, X. Ou, H. Wu, D. Feng, X. Hui Chen, and Y. Zhang, "Black phosphorus field-effect transistors," *Nat. Nanotechnol.* **9**, 372–377 (2014).
30. M. Naguib, M. Kurtoglu, V. Presser, J. Lu, J. Niu, M. Heon, L. Hultman, Y. Gogotsi, and M. W. Barsoum, "Two-dimensional nanocrystals produced by exfoliation of  $\text{Ti}_3\text{AlC}_2$ ," *Adv. Mater.* **23**, 4248–4253 (2011).
31. E. Hendry, P. J. Hale, J. Moger, A. K. Savchenko, and S. A. Mikhailov, "Coherent nonlinear optical response of graphene," *Phys. Rev. Lett.* **105**, 097401 (2010).
32. R. Wang, H. C. Chien, J. Kumar, N. Kumar, H. Y. Chiu, and H. Zhao, "Third-harmonic generation in ultrathin films of  $\text{MoS}_2$ ," *ACS Appl. Mater. Interfaces* **6**, 314–318 (2014).
33. S. Lu, C. Zhao, Y. Zou, S. Chen, Y. Chen, Y. Li, H. Zhang, S. Wen, and D. Tang, "Third order nonlinear optical property of  $\text{Bi}_2\text{Se}_3$ ," *Opt. Express* **21**, 2072–2082 (2013).
34. Y. Q. Ge, S. Chen, Y. J. Xu, Z. L. He, Z. M. Liang, Y. X. Chen, Y. F. Song, D. Y. Fan, K. Zhang, and H. Zhang, "Few-layer selenium-doped black phosphorus: synthesis, nonlinear optical properties and ultrafast photonics applications," *J. Mater. Chem. C* **5**, 6129–6135 (2017).
35. X. T. Jiang, S. X. Liu, W. Y. Liang, S. J. Luo, Z. L. He, Y. Q. Ge, H. D. Wang, R. Cao, F. Zhang, Q. Wen, J. Q. Li, Q. L. Bao, D. Y. Fan, and H. Zhang, "Broadband nonlinear photonics in few-layer MXene  $\text{Ti}_3\text{C}_2\text{T}_x$  ( $T = \text{F}, \text{O}, \text{or OH}$ )," *Laser Photon. Rev.* **12**, 1700229 (2017).
36. Q. L. Bao, H. Zhang, Y. Wang, Z. Ni, Y. Yan, Z. X. Shen, K. P. Loh, and D. Y. Tang, "Atomic layer graphene as saturable absorber for ultrafast pulsed laser," *Adv. Funct. Mater.* **19**, 3077–3083 (2009).
37. Z. Sun, T. Hasan, F. Torrisi, D. Popa, G. Privitera, F. Wang, F. Bonaccorso, D. M. Basko, and A. C. Ferrari, "Graphene mode-locked ultrafast laser," *ACS Nano* **4**, 803–810 (2010).
38. H. Liu, A. P. Luo, F. Z. Wang, R. Tang, M. Liu, Z. C. Luo, W. C. Xu, C. J. Zhao, and H. Zhang, "Femtosecond pulse erbium-doped fiber laser by a few-layer  $\text{MoS}_2$  saturable absorber," *Opt. Lett.* **39**, 4591–4594 (2014).
39. K. Wu, X. Zhang, J. Wang, and J. Chen, "463-MHz fundamental mode-locked fiber laser based on few-layer  $\text{MoS}_2$  saturable absorber," *Opt. Lett.* **40**, 1374–1377 (2015).
40. A. P. Luo, M. Liu, X. D. Wang, Q. Y. Ning, W. C. Xu, and Z. C. Luo, "Few-layer  $\text{MoS}_2$ -deposited microfiber as highly nonlinear photonic device for pulse shaping in a fiber laser [Invited]," *Photon. Res.* **3**, A69–A78 (2015).
41. R. I. Woodward, R. C. T. Howe, G. Hu, F. Torrisi, M. Zhang, T. Hasan, and E. J. R. Kelleher, "Few-layer  $\text{MoS}_2$  saturable absorbers for short-pulse laser technology: current status and future perspectives," *Photon. Res.* **3**, A30–A42 (2015).
42. P. Yan, R. Lin, S. Ruan, A. Liu, and H. Chen, "A 2.95 GHz, femtosecond passive harmonic mode-locked fiber laser based on evanescent field interaction with topological insulator film," *Opt. Express* **23**, 154–164 (2015).
43. D. Mao, B. Jiang, X. Gan, C. Ma, Y. Chen, C. Zhao, H. Zhang, J. Zheng, and J. Zhao, "Soliton fiber laser mode locked with two types of film-based  $\text{Bi}_2\text{Te}_3$  saturable absorbers," *Photon. Res.* **3**, A43–A46 (2015).
44. Y. Chen, M. Wu, P. H. Tang, S. Q. Chen, J. Du, G. B. Jiang, Y. Li, C. J. Zhao, H. Zhang, and S. C. Wen, "The formation of various multi-soliton patterns and noise-like pulse in a fiber laser passively mode locked by a topological insulator based saturable absorber," *Laser Phys. Lett.* **11**, 055101 (2014).
45. P. G. Yan, R. Y. Lin, H. Chen, H. Zhang, A. J. Liu, H. P. Yang, and S. C. Ruan, "Topological insulator solution filled in photonic crystal fiber for passive mode-locked fiber laser," *IEEE Photon. Technol. Lett.* **27**, 951–954 (2015).
46. D. Li, H. Jussila, L. Karvonen, G. Ye, H. Lipsanen, X. Chen, and Z. Sun, "Polarization and thickness dependent absorption properties of black phosphorus: new saturable absorber for ultrafast pulse generation," *Sci. Rep.* **5**, 15899 (2015).
47. Y. Chen, G. Jiang, S. Chen, Z. Guo, X. Yu, C. Zhao, H. Zhang, Q. Bao, S. Wen, D. Tang, and D. Fan, "Mechanically exfoliated black phosphorus as a new saturable absorber for both Q-switching and mode-locking laser operation," *Opt. Express* **23**, 12823–12833 (2015).
48. Z. C. Luo, M. Liu, Z. N. Guo, X. F. Jiang, A. P. Luo, C. J. Zhao, X. F. Yu, W. C. Xu, and H. Zhang, "Microfiber-based few-layer black phosphorus saturable absorber for ultra-fast fiber laser," *Opt. Express* **23**, 20030–20039 (2015).
49. Z. Q. Luo, M. Zhou, D. Wu, C. Ye, J. Weng, J. Dong, H. Xu, Z. Cai, and L. Chen, "Graphene-induced nonlinear four-wave-mixing and its application to multiwavelength Q-switched rare-earth-doped fiber lasers," *J. Lightwave Technol.* **29**, 2732–2739 (2011).
50. H. Zhang, S. Virally, Q. Bao, L. K. Ping, S. Massar, N. Godbout, and P. Kockaert, "Z-scan measurement of the nonlinear refractive index of graphene," *Opt. Lett.* **37**, 1856–1858 (2012).
51. R. Ciesielski, A. Comin, M. Handloser, K. Donkers, G. Piredda, A. Lombardo, A. C. Ferrari, and A. Hartschuh, "Graphene near-degenerate four-wave mixing for phase characterization of broadband pulses in ultrafast microscopy," *Nano Lett.* **15**, 4968–4972 (2015).
52. Y. Wu, B. C. Yao, Q. Y. Feng, X. L. Cao, X. Y. Zhou, Y. J. Rao, Y. Gong, W. L. Zhang, Z. G. Wang, Y. F. Chen, and K. S. Chiang, "Generation of cascaded four-wave-mixing with graphene-coated microfiber," *Photon. Res.* **3**, A64–A68 (2015).
53. G. Brambilla, V. Finazzi, and D. J. Richardson, "Ultra-low-loss optical fiber nanotapers," *Opt. Express* **12**, 2258–2263 (2004).
54. K. Kashiwagi and S. Yamashita, "Deposition of carbon nanotubes around microfiber via evanescent light," *Opt. Express* **17**, 18364–18370 (2009).

55. Z. C. Luo, M. Liu, H. Liu, X. W. Zheng, A. P. Luo, C. J. Zhao, H. Zhang, S. C. Wen, and W. C. Xu, "2 GHz passively harmonic mode-locked fiber laser by a microfiber-based topological insulator saturable absorber," *Opt. Lett.* **38**, 5212–5215 (2013).
56. O. Schwelb, "Transmission, group delay, and dispersion in single-ring optical resonators and add/drop filters—a tutorial overview," *J. Lightwave Technol.* **22**, 1380–1394 (2004).
57. X. S. Jiang, L. M. Tong, G. Vienne, X. Guo, A. Tsao, Q. Yang, and D. R. Yang, "Demonstration of optical microfiber knot resonators," *Appl. Phys. Lett.* **88**, 223501 (2006).
58. M. Nakazawa, K. Tamura, and E. Yoshida, "Supermode noise suppression in a harmonically mode-locked fibre laser by self-phase modulation and spectral filtering," *Electron. Lett.* **32**, 461–463 (1996).
59. E. Yoshida and M. Nakazawa, "Low-threshold 115-GHz continuous-wave modulational-instability erbium-doped fiber laser," *Opt. Lett.* **22**, 1409–1411 (1997).
60. J. Schröder, D. Alasia, T. Sylvestre, and S. Coen, "Dynamics of an ultrahigh-repetition-rate passively mode-locked Raman fiber laser," *J. Opt. Soc. Am. B* **25**, 1178–1186 (2008).
61. X. S. Jiang, Q. Yang, G. Vienne, Y. H. Li, L. M. Tong, J. Zhang, and L. Hu, "Demonstration of microfiber knot laser," *Appl. Phys. Lett.* **89**, 143513 (2006).
62. W. Fan, J. L. Gan, Z. S. Zhang, X. M. Wei, S. H. Xu, and Z. M. Yang, "Narrow linewidth single frequency microfiber laser," *Opt. Lett.* **37**, 4323–4325 (2012).